



JOURNAL OF
APPLIED
CRYSTALLOGRAPHY

Volume 55 (2022)

Supporting information for article:

Unveiling the anisotropic fractal magnetic domain structure in bulk crystal of antiskyrmion host (Fe,Ni,Pd)₃P by small-angle neutron scattering

Kosuke Karube, Victor Ukleev, Fumitaka Kagawa, Yoshinori Tokura, Yasujiro Taguchi and Jonathan S. White

S1. Experimental details of MFM measurements

In the MFM measurements, a plate-shaped bulk single crystal with a flat (001) surface was used, as shown in Fig. S1(b). Magnetic fields were applied perpendicular to the sample plate using cylindrical Nd-Fe-B permanent magnets as illustrated schematically in Fig. S1(a). Figures S1(c-j) show MFM images of fractal magnetic domain patterns at various magnetic fields. As the magnetic field is applied, the dark stripe domains shrink at 0.13 T and change to square, letter N- and letter J-shaped domains at 0.18 T. Upon further increasing the field from 0.22 T to 0.31 T, the main domains become smaller and rounder (or triangular), and all the bubble-like domains finally disappear above 0.35 T to enter a single domain state. After the magnetic field of 0.37 T is removed, many square-shaped domains remain at zero field, different from the initial stripe domains.

S2. Box-counting analysis of MFM image

The fractal dimension of the MFM image at zero field was calculated using a box-counting method (Falconer, 1990; Smith *et al.*, 1996; Han *et al.*, 2002; Lisovskii *et al.*, 2004), as shown in Fig. S2. As this method requires an image with a sufficiently wide scale and high resolution, here a high-resolution MFM image with a size of $30\ \mu\text{m} \times 30\ \mu\text{m}$ (1113×1113 pixels) [Fig. S2(a)] was used. For the image processing and box counting, the software ImageJ (Ver. 1.53k) was used. The MFM image was grey-scaled and binarized to extract the domain boundaries. As schematically shown in Fig. S2(b), the domain boundaries are covered with a grid of boxes of side length s , and the number of boxes N intercepted by the domain boundaries is counted for various s . The fractal dimension (box-counting dimension) D is defined as,

$$D = -\lim_{s \rightarrow 0} \frac{\log[N(s)]}{\log(s)}, \quad (\text{S1})$$

and obtained from the slope of the log-log plot of $N(s)$. Figure S2(c) shows the result of the log-log plot of $N(s)$ for the MFM image. The slope at the large s region is close to $D = 2$ (dotted line), but this is the dimension of the whole image plane as the selected box sizes are too large to resolve the domain boundaries, thus this segment should be excluded. A linear slope of $D = 1.29(1)$ can fit the data points in the small s region between $s = 54\ \text{nm}$ (2 pixels) and $323\ \text{nm}$ (12 pixels), over which fractality can be defined. Note that this length scale is comparable to that probed by SANS.

S3. Experimental details of SANS measurements

In order to cover a wide q range, SANS patterns were taken in two configurations with different collimator and detector distances, as shown in Figs. S3(a-c) and S3(d-f), respectively. Figures S3(a, d) show SANS patterns at 300 K and 0 T before background subtraction. Figures S3(b, e) show SANS patterns in the fully polarized state at 0.8 T, which show asymmetric streaks due to specular reflection

of neutrons from sharp sample edges as shown in the photo [Fig. S3(g)]. The SANS patterns at 0 T after background subtraction using the data at 0.8 T are shown in Figs. S3(c, f). While the SANS signal derived from magnetic domains is strong compared to the background signal, all of the analysis presented in the main text was done on the SANS data obtained after background subtraction.

S4. Rocking scans of SANS measurements

Figure S4 shows the rocking scans around the vertical $[\bar{1}10]$ direction (rocking angle ω) and the horizontal $[110]$ direction (rocking angle χ) in the range from -3° to 3° . In both orientations, the rocking curves are very sharp (FWHM $\sim 0.5^\circ$). This confirms that the cross-shaped SANS pattern is present only within the tetragonal basal plane with a long correlation length along the easy $[001]$ direction.

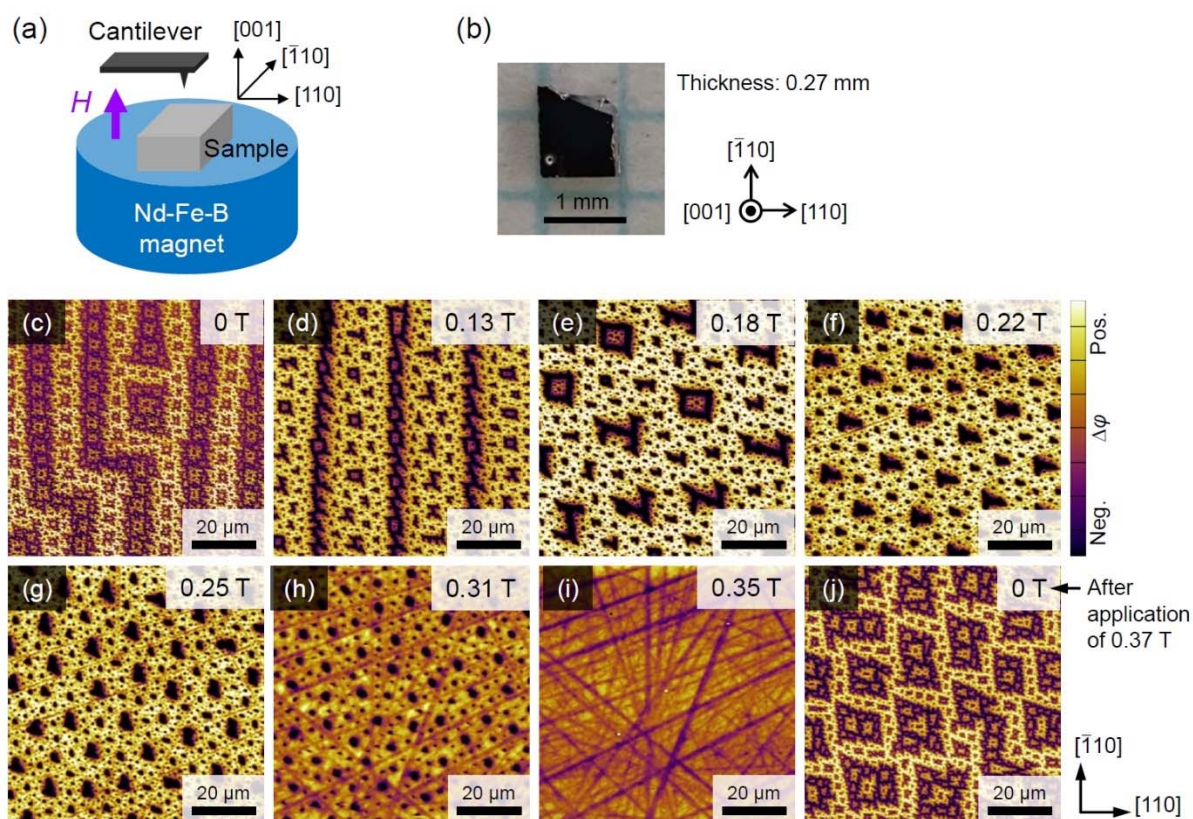


Figure S1 Details of the MFM measurement. (a) Schematic of the experimental setup. (b) Photo of the bulk single crystal of $(\text{Fe}_{0.63}\text{Ni}_{0.30}\text{Pd}_{0.07})_3\text{P}$ used for the MFM measurement. (c-j) MFM phase images at room temperature and at various magnetic fields. A number of straight lines observed at high fields are due to polishing scratches left on the sample surface.

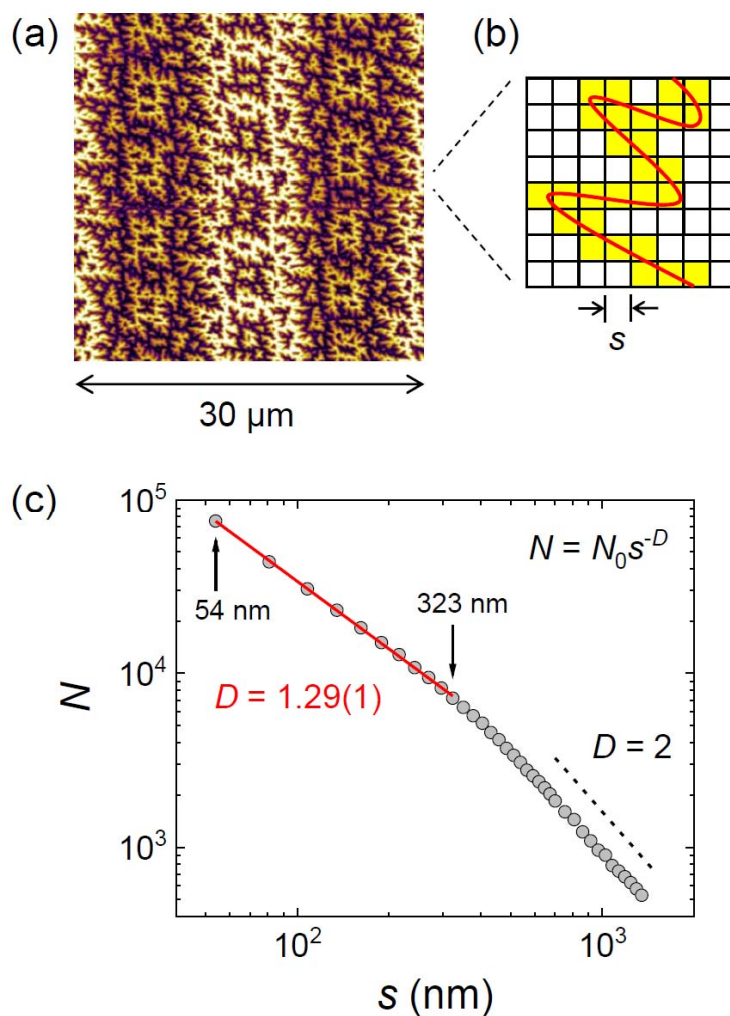


Figure S2 Fractal analysis of the MFM magnetic domain pattern. (a) MFM image at room temperature and zero field [the same as Fig. 2(b) in the main text] used for the analysis. (b) Schematic of box-counting analysis. The number of yellow boxes N intercepted by the red domain boundary is counted for various box sizes s . (c) Log-log plot of $N(s)$ for the MFM image. The fractal dimension $D = 1.29(1)$ is obtained from the slope (red line) over the length region between 323 nm and 54 nm as indicated with the arrows. The slope of $D = 2$ is also indicated with the dotted line.

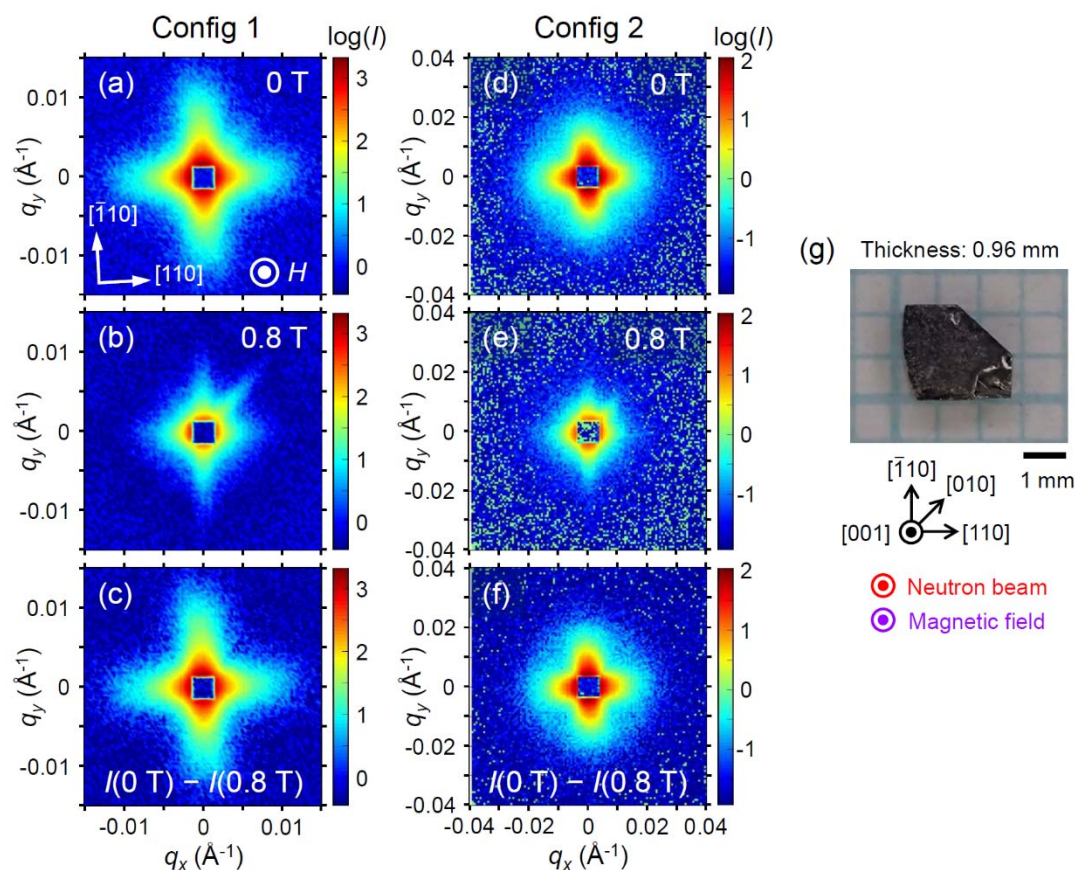


Figure S3 Details of the SANS measurement. (a-f) SANS patterns at 300 K in two different configurations: Config 1 (detector 20 m, collimator 18 m) and Config 2 (detector 8 m, collimator 8 m). Panels (a, d) and (b, e) are SANS patterns without background subtraction recorded at 0 T (multi-domain state) and 0.8 T (fully polarized state), respectively. Panels (c, f) show the results of the subtraction of the background obtained at 0.8 T from the data at 0 T and represent the purely magnetic scattering component at 0 T. (g) Photo of the bulk single crystal of $(\text{Fe}_{0.63}\text{Ni}_{0.30}\text{Pd}_{0.07})_3\text{P}$ used for the SANS measurement.

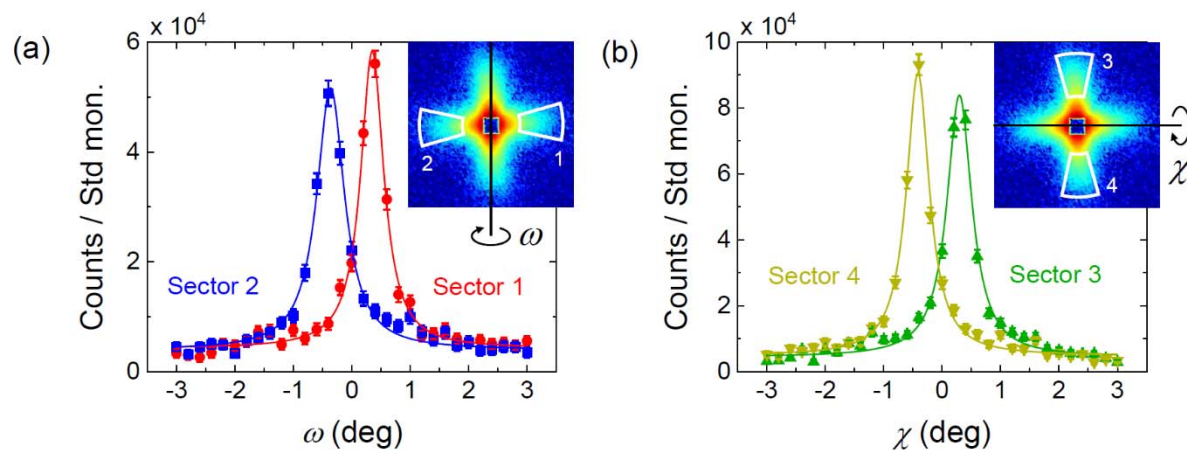


Figure S4 Rocking scans of the magnetic SANS pattern at 300 K and zero field. (a) Rocking curves for the regions 1 and 2 indicated in the inset during the rotation around the vertical axis (rocking angle ω). (b) Rocking curves for the regions 3 and 4 indicated in the inset during the rotation around the horizontal axis (rocking angle χ). Data points are fitted to the Lorentzian function with a full width at half maximum (FWHM) of $\sim 0.5^\circ$ (solid lines).